

RESONANCE MODEL IN NUCLEON-ANTINUCLEON
ANNIHILATION

G. Cocho Gil

Princeton University, Princeton N.J. *

(Recibido: 20 Diciembre de 1962)

RESUMEN

The $\bar{N}N$ annihilation at rest is analyzed assuming the final state interactions are so strong, that instead of a n particle phase space, we have actually a 2 particle phase space. Considering as particles the π , ρ and ω "particles", and taking in account only the one nucleon exchange diagrams, expressions are derived for the charge multiplicity distribution and for the one pion energy spectrum. These expressions are function of the $\bar{N}N\pi$, $\bar{N}N\rho$ and $\bar{N}N\omega$ "effective" coupling constants. We use these as parameters which are chosen to fit the experimental charge multiplicity distribution. When these values are used in the expression for the energy spectrum, we obtain a good agreement with the experimental data, except that our model yields sharp peaks, which are not evident in the experimental data. (In our model, these peaks come from the processes $\bar{N} + N \rightarrow \pi + \rho$, $\bar{N} + N \rightarrow \pi + \omega$).

* Present address: Instituto de Física, Universidad Nacional de México.

I. INTRODUCCION

Since the discovery of the antiproton in 1955¹ and the discovery of the antineutron soon afterwards², a large amount of experimental work has been carried out on the nucleon-antinucleon interaction with counters, emulsions and bubble chambers³.

The results of these investigations show two peculiar facts:

- 1.- Large $\bar{N}N$ scattering and annihilation cross sections.
- 2.- Larger multiplicities than the ones computed using the statistical model⁴, if a reasonable radius of interaction i.e. $1/\mu$ is assumed.

In an attempt to avoid the uncomfortably large interaction radius, several phenomenological models have been assumed:

Koba and Takeda⁵ have assumed the $\bar{N}N$ annihilation process occurs in two steps: First the $\bar{N}N$ annihilation occurs between the cores with the emission of 2.2 pions on the average and in a such a short time the pionic clouds are left unaffected; afterward, the clouds break up and produce extra pions (2.6 on the average). Using a core radius of $2/3\mu$, they are able to fit the total and absorptive cross section and the pion multiplicity. However, with this set of values the energy spectrum is peaked in a larger energy than the one observed experimentally.

Ball and Chew⁶ have attacked the problem in a similar way. They replace the core by an ingoing wave boundary condition, which represents the large probability of annihilation if the two particles come close together. It was found, that their results were insensitive to the localization of the boundary for intermediate energies (50-100 MeV). They treated only the problem of the cross section and were able to fit the experimental data in that region.

Cook and Lepore⁷ computed the pion multiplicities and energy spectrum, including:

a.- The approximate energy dependence of the matrix elements, which are neglected in the Fermi statistical model.

b.- The results of the calculation of Ball and Chew with respect to the partial

waves involved in annihilation. They characterized the reaction by an interaction range and a coupling strength and fixed these two parameters by fitting the multiplicity and energy spectrum.

Other authors⁸ have tried to include strong final state interactions in the statistical model, in order to enhance the multiplicity without much success.

The main idea behind this work is to study the $\bar{N}N$ annihilation process, using a model that is in a certain sense the opposite point of view to the statistical model. In the statistical model, one ignores the energy dependence of the matrix elements and considers only the variation of the phase space. However, we will consider the extreme point of view that the pion-pion correlations (final state interactions) are so strong that instead of a n particles phase space, we have actually a 2 or 3 particles phase space. We will consider as particles: π , ρ and ω , and we will study the case when in the annihilation only two of them are present. (Although, there are another resonances such as the η , ρ , since their mass is lower than the ρ and ω masses, and they have a very small width, we expect by phase space considerations, their contribution is going to be less important.) Out of ignorance, we will consider only the one nucleon exchange diagrams, and we will study the multiplicity distribution and the one pion energy spectrum in the $\bar{N}N$ annihilation at rest, using parameters what are very closely related to the $\bar{N}N\pi$, $\bar{N}N\rho$ and $\bar{N}N\omega$ coupling constants.

II. ONE NUCLEON EXCHANGE DIAGRAMS, VERTEX FUNCTIONS AND SPIN SUMS

In studying the process $\bar{N} + N \rightarrow n\pi$, we may separate the contributions coming from the one nucleon exchange diagrams and the ones coming from the remaining diagrams (Fig. 1).

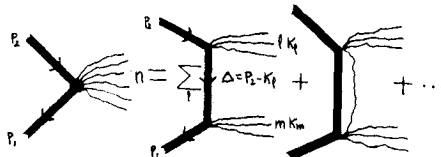


Fig. 1

$$K_l = \sum_{i=1}^l k_i \quad K_m = \sum_{i=l+1}^n k_i$$

\sum_l means sum over all the possible partitions of n in two numbers: l and $m = n - l$.

For the process $\bar{N} + N \rightarrow n\pi$ we may write the matrix element.

$$\begin{aligned} M_{n\pi; \bar{N}N} &= \prod_{i=1}^n (2\omega_i)^{1/2} \bar{v}(p_1) \langle k_{1\alpha} \dots k_{n\omega}^{(-)} | f | p_2 \rangle \left(\frac{p_{20}}{m} \right)^{1/2} = \\ &= \bar{v}(p_1) \mathfrak{M}_{n\pi; \bar{N}N} u(p_2) \end{aligned} \quad (2.1)$$

Similarly, we may write

$$\begin{aligned} M_{Nn\pi; N} &= \prod_{i=1}^n (2\omega_i)^{1/2} u(p_1) \langle p_2 k_{1\alpha} \dots k_{n\omega}^{(-)} | f | 0 \rangle \left(\frac{p_{20}}{m} \right)^{1/2} = \\ &= u(p_1) \mathfrak{M}_{Nn\pi; N} u(p_2) \end{aligned} \quad (2.2)$$

(Of course, $\mathfrak{M}_{Nn\pi; N}$ is the analytical continuation of $\mathfrak{M}_{n\pi; \bar{N}N}$, with $f = f(0)$ and $\bar{f} = \bar{f}(0)$, $f(x)$, $\bar{f}(x)$ being the Dirac current operators obeying

$$\left[\gamma_\mu \frac{\partial}{\partial x_\mu} + m \right] \psi(x) = f(x) \quad \left[-\gamma_\mu^T \frac{\partial}{\partial x_\mu} + m \right] \bar{\psi}(x) = \bar{f}(x) \quad (2.3)$$

If only the one nucleon exchange diagrams are considered, we have

$$M_{n\pi; \bar{N}N} = \sum_l \bar{v}(p_1) \mathfrak{M}_{l\pi; \bar{N}N} \frac{1}{i(p_2 - \not{x}_l) + m} \mathfrak{M}_{N(n-l); N} u(p_2) \quad (2.4)$$

with $1 < l < n - 1$

Since the mass of the nucleon in the propagator takes only non physical

values, in 1-4 the m_N are the analytical continuation in the nucleon mass to this non physical values.

In this work we will consider values of n (number of pions) such that $3 < n < 6$. Due to the presence of the $2\pi, 3\pi$ resonances 9,10 , we will consider only $1, m = 1, 2, 3$. Therefore, we have to study the following partitions of the final state:

$$\bar{N} + N \rightarrow 2\pi + \pi, 3\pi + \pi, 2\pi + 2\pi, 2\pi + 3\pi, 3\pi + 3\pi \quad (2.5)$$

Vertex Functions

We need to know something about the structure of the vertexes $\bar{N}N\pi, \bar{N}N2\pi$ and $\bar{N}N3\pi$.

A.- $\bar{N}N\pi$.

For this matrix element, we have

$$M_{\pi_\alpha; \bar{N}N} = \left(\frac{P_{10} P_{20}}{m^2} \right)^{1/2} \langle 0 | J_\alpha | \bar{P}_1 P_2 \rangle = G \bar{v}(p_1) \gamma_5 \tau_\alpha U(p_2) \quad (2.6)$$

where $J_\alpha = J_\alpha(0)$, $J_\alpha(x)$ is the current operator for the pion field, obeying the equation

$$(\mu^2 - \square) \phi_\alpha(x) = J_\alpha(x) \quad (2.7)$$

$\phi_\alpha(x)$ is the field for the pion of isotopic index α , G is the $\bar{N}N\pi$ coupling constant and γ_5, τ_α are the usual Dirac and Pauli matrices. (Due to the non physical value of the mass in the propagator, the value of G may be different from the mass shell value).

The same considerations apply to the vertex functions to be discussed next.

B.- $\bar{N}N2\pi$.

We write the matrix element as

$$M_{\pi_\alpha \pi_\beta; \bar{N}N} = (4\omega_1 \omega_2)^{1/2} \bar{v}(p_1) \langle k_{1\alpha} k_{2\beta}^{(-)} | f | p_2 \rangle \left(\frac{p_{20}}{m} \right) \quad (2.8)$$

Due to the existence of the 2π resonance, in the state with quantum numbers $J=1, T=1$; it is reasonable to assume that the main contribution comes from that state. The relevant part of the matrix element has the structure

$$M_{\pi_a \pi_\beta; \bar{N}N} = 1/2 (k_1 - k_2)_\mu (-) \bar{v}(p_1) 1/2 [\tau_a, \tau_\beta] [a_1 i\gamma_\mu + b_1 (p_1 - p_2)_\mu] u(p_2) \quad (2.9)$$

The invariant functions a_1, b_1 depend on t , where $t = -(k_1 + k_2)^2 = -(p_1 + p_2)^2$.

We define A_1, B_1 by

$$a_1 \equiv A_1 e^{\Delta(t)} \quad b_1 \equiv B_1 e^{\Delta(t)} \quad (2.10)$$

where $\Delta(t)$ is the usual integral over the $\pi - \pi$ phase shift;

$$\Delta(t) = \frac{t}{\pi} \int_4^{\infty} \frac{dt' \delta\pi(t')}{\mu^2 t' (t' - t)} \quad (2.11)$$

Here $\delta_{\pi\pi}$ is the resonant $J=1, T=1$ pion pion phase shift. We expect A_1, B_1 to be slowly variant functions of t in the region around the resonance and therefore, we may approximate them by constants in that region.

Following Frazer and Fulco¹¹, we may write $e^{\Delta(t)}$ in the Breit-Wigner form consistent with unitarity and with the correct behavior at threshold:

$$e^{\Delta(t)} \sim \frac{i}{t - t_v - i\Gamma_1 \frac{(t-4)^{3/2}}{t^{1/2}}} \quad (2.12)$$

where t_v is the position of the 2π resonance and $\Gamma_1 \frac{(t_v-4)^{3/2}}{t_v^{1/2}}$ is the halfwidth.

C.- $\bar{N}N3\pi$.

In this case, we write the matrix element

$$M_{\pi_\alpha \pi_\beta \pi_\gamma; \bar{N}N} = (8\omega_1 \omega_2 \omega_3)^{1/2} \bar{v}(p_1) \langle k_{1\alpha} k_{2\beta} k_{3\gamma}^{(-)} | f | p_2 \rangle \left(\frac{p_{20}}{m} \right)^{1/2} \quad (2.13)$$

We will assume that the $1^- T = 0$ 3π resonance (10a) may be considered as dominating the 3π contribution. The pertinent matrix element has the structure:

$$M_{\pi_\alpha \pi_\beta \pi_\gamma; \bar{N}N} = i \epsilon_{\mu\nu\lambda\tau} k_1^\nu k_2^\lambda k_3^\tau \epsilon^{\alpha\beta\gamma} \bar{v}(p_1) [a_2 i\gamma_\mu + b_2 (p_1 - p_2)_\mu] U(p_2) \quad (2.14)$$

The invariant functions a_2, b_2 depend upon the invariants t, t_{ij}, s_{ij} . (However, only five of them are independent); where

$$\begin{aligned} t &= -(p_1 + p_2)^2 = -(k_1 + k_2 + k_3)^2 \\ t_{ij} &= -(k_i + k_j)^2 \\ s_{ij} &= -(p_i + k_j)^2 \end{aligned} \quad (2.15)$$

In 2.14, $\epsilon^{\alpha\beta\gamma}$ projects $T = 0$ and $-i \epsilon_{\mu\nu\lambda\tau} k_1^\nu k_2^\lambda k_3^\tau$ the 1^- state. As in Blankenbeclerwork¹², we define A_2, B_2 by

$$\begin{bmatrix} a_2 \\ b_2 \end{bmatrix} = \begin{bmatrix} A_2 \\ B_2 \end{bmatrix} \exp [\Delta(t_{12}) + \Delta(t_{13}) + \Delta(t_{23})] D(t)^{-1} = \exp \sum \Delta_{ij} x D(t)^{-1} \quad (2.16)$$

The function $\exp \sum \Delta_{ij}$ has the phase shift due to each pion pair resonantly rescattering and $D(t)^{-1}$ contains the effects of the intrinsic 3π final state interaction.

From the existence of the 3π resonance (ω particle), we know $D(t)^{-1}$ behaves

as a resonance near $t = t_s$, where t_s is the position of the observed experimental resonance.

We choose for $D(t)^{-1}$ the resonance form

$$\frac{1}{D(t)} \sim \frac{1}{t - t_s - i\Gamma_2 G_3(t)} \quad (2.17)$$

This form is consistent with unitarity and has the correct behavior at threshold. $G_3(t)$ is the "effective" phase space and $\Gamma_2 G_3(t_s)$ is the halfwidth. We hope that A_2, B_2 are slowly variant functions of t around the resonance, and so we may replace them by constants in that region. Also, we assume we may drop the dependence on the other invariants.

From the preceding considerations, we see that if the 1^- state dominates both in $M_{2\pi, \bar{N}N}$ and $M_{3\pi, \bar{N}N}$, the basic structure of these vertices is the one corresponding to a $\bar{N}-N$ -vector particle coupling. For the resonant $2\pi [3\pi]$ state, $1/2 (k_1 - k_2) [-i\epsilon_{\mu\nu\lambda\tau} k_1^\nu k_2^\lambda k_3^\tau]$ plays the role of polarization vector.

The basic structure of the $\bar{N}N$ annihilation process in the model that we are using is given by the lowest order perturbation diagrams for the processes:

$$\begin{aligned} \bar{N} + N &\rightarrow \pi + \rho \\ \bar{N} + N &\rightarrow \pi + \omega \end{aligned} \quad \left. \vphantom{\begin{aligned} \bar{N} + N \\ \bar{N} + N \end{aligned}} \right\} \text{ scalar + vector} \quad (2.18)$$

$$\begin{aligned} \bar{N} + N &\rightarrow \rho + \rho \\ \bar{N} + N &\rightarrow \rho + \omega \\ \bar{N} + N &\rightarrow \omega + \omega \end{aligned} \quad \left. \vphantom{\begin{aligned} \bar{N} + N \\ \bar{N} + N \\ \bar{N} + N \end{aligned}} \right\} \text{ vector + vector} \quad (2.19)$$

Therefore, we need to write up the matrix elements for the lowest order perturbation diagrams of the processes $\bar{N} + N \rightarrow S + V$, $\bar{N} + N \rightarrow V + V$ and to evaluate the spin sums (average over the initial nucleon-antinucleon spin states). S (V) will denote a scalar (vector) particle.

$$\bar{N} + N \rightarrow S + V$$

The relevant diagrams are

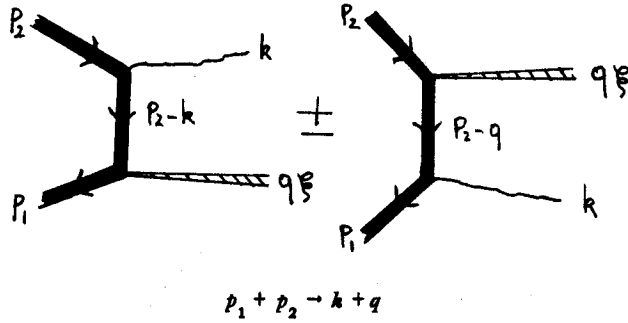


Figura 2

Where p_2 (p_1) is the momentum 4-vector of the nucleon (antinucleon), $k(q)$ is the momentum 4-vector of the scalar (vector particle) and ξ is the vector particle polarization such that $\xi \cdot q = 0$.

The \pm sign will depend on the isotopic structure.

If M_{\pm}^s denotes this matrix element, we have

$$M_{\pm}^s = \frac{Gi}{(p_2 - k)^2 + m^2} \bar{v}(p_1) [-\alpha\gamma_{\mu} + ib(p_1 - p_2 + k)_{\mu}] \not{k} \gamma_5 u(p_2) \xi_{\mu} \pm$$

$$\pm \frac{Gi}{(p_1 - k)^2 + m^2} \bar{v}(p_1) [-\not{k} \gamma_5 \gamma_{\mu} a + ib(p_1 - p_2 - k)_{\mu} \not{k} \gamma_5] u(p_2) \xi_{\mu} \quad (2.20)$$

In the case we are interested (nucleon-antinucleon annihilation at rest), we obtain after averaging over the initial spin states

$$\frac{1}{4} \sum_{\text{spin}} |M_{\pm}^s|^2 = \frac{8G^2}{(4m^2 - \mu_v^2 - \mu_s^2)^2} |\alpha|^2 [k^2 \xi \cdot \xi - \frac{\mu_v^2}{4m^2} (\xi \cdot k)^2] \quad (2.21)$$

$$1/4 \sum_{\text{spin}} |M_{\pm}^{\epsilon}|^2 = \frac{8G^2}{(4m^2 - \mu_s^2 - \mu_v^2)} |a - b k_0|^2 (\xi \cdot k)^2 \quad (2.22)$$

$$\bar{N} + N \rightarrow V_1 + V_2$$

Defining V_1, V_2 as the vector particles, the pertinent diagrams are

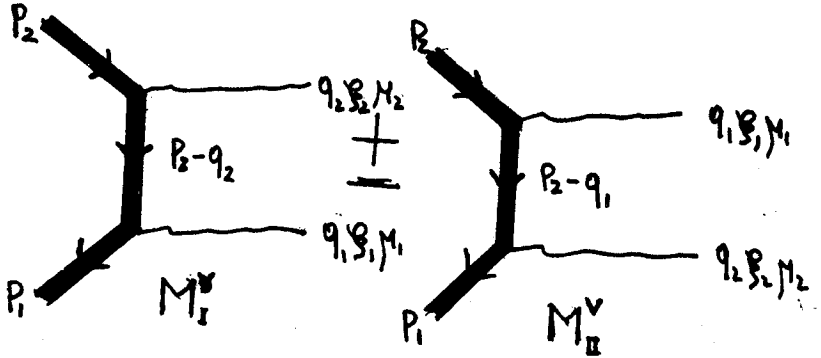


Figura 3

where $K = p_1 + p_2 = q_1 + q_2$ and q_i, ξ_i, μ_i are the momentum 4-vector, polarization vector and mass of the vector particle V_i . We require that $q_{(i)} \cdot \xi_{(i)} = 0$. If a_i, b_i are the coupling constants for the vertex $\bar{N}NV_i$ using the Dirac equation and the anticommutation properties of the γ_s , we have

$$\begin{aligned} M_I^V = & \frac{1}{(p_2 - q_2)^2 + m^2} \bar{v}(p_1) \{ -a_1 a_2 [i\gamma_\mu 2p_{2\nu} - i\gamma_\mu \not{q}_2 \gamma_\nu] + \\ & + ib_1 a_2 (p_1 - p_2 + q_2)_\mu [2ip_{2\nu} - i\not{q}_2 \gamma_\nu] + ia_1 b_2 \gamma_\mu (p_1 - p_2 - q_1)_\nu (-2m - i\not{q}_2) + \\ & + b_1 b_2 (p_1 - p_2 + q_2)_\mu (p_1 - p_2 - q_1)_\nu (-2m - i\not{q}_2) \} u(p_2) \xi_1^\mu \xi_2^\nu \end{aligned} \quad (2.23)$$

We get M_{II}^{ν} from M_I^{ν} by making the substitution $\mu \rightarrow \nu, q_1 \rightarrow q_2, a_1 b_1 \rightarrow a_2, b_2$.

If M_{\pm}^{ν} denotes $M_I^{\nu} \pm M_{II}^{\nu}$, we obtain when we average over the initial spin states

$$\frac{1}{4} \sum_{\text{spin}} |M_{+}^{\nu}|^2 = \frac{2a_1^2 a_2^2}{(4m^2 - \mu_1^2 - \mu_2^2)^2} \frac{1}{m^2} [-i \epsilon_{\mu\nu\lambda\tau} \xi_{1\mu} \xi_{2\nu} Q \lambda K_{\tau}]^2 \quad (2.24)$$

where

$$Q = 1/2 (q_1 - q_2)$$

In our problem we will need M_{-}^{ν} only for the particular case $\mu_1 = \mu_2 = \mu$. For this case we obtain

$$\begin{aligned} \frac{1}{4} \sum_{\text{spin}} |M_{-}^{\nu}|^2 &= \frac{2}{(4m^2 - 2\mu^2)^2} \{ |2a^2 + 2mba|^2 [\xi_{1\alpha} \xi_{1\beta} (\xi_{2\gamma} \cdot q_1)^2 + \xi_{2\alpha} \xi_{2\beta} (q_2 \cdot \xi_1)^2] \\ &+ \xi_{1\alpha} \xi_{2\alpha} q_2 \cdot \xi_1 q_1 \cdot \xi_2 [-2 |2a^2 + 2mba|^2 - 8 \vec{Q}^2 b^2 a^2 + 4a^2(2a^2 + 2mba)] \\ &+ 4\vec{Q}^2 a^4 (\xi_1 \cdot \xi_2) + 4(q_2 \cdot \xi_1)(q_1 \cdot \xi_2) [b^4 \vec{Q}^2 - (2a^2 + 2mba) b^2] \} \quad (2.25) \end{aligned}$$

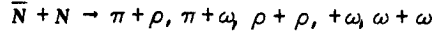
III. DECAY RATES AND ONE PION ENERGY SPECTRA

In this section we proceed to compute the annihilation rate (probability of transition of the $\bar{N}N$ system to the pertinent final channel), and the one pion energy spectrum.

By $W_j^i(pp) [W_j^i(\bar{p}n)]$, we will denote the probability of transition of the $\bar{p}p$ [$\bar{p}n$] system into i pions, j of them charged. $\sum_i W_j^i$ is the charge multiplicity distribution. $\sum_{ij} W_j^i$ is the probability of decaying in i pions. $\sum_{ij} W_j^i$ is the total rate.

We may define similar quantities for the energy spectrum: $W_j^i(k; \bar{p}p)$ will denote the probability that the $\bar{p}p$ system decays into i pions, j of them charged, and one of the positive pions with momentum k . (We may define similar quantities for the negative or neutral pions and for the $\bar{p}n$ system).

As discussed in the first chapter we will assume the basic structure is given by the reactions.



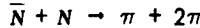
In order to simplify the nomenclature, the $\bar{N}N, \rho\pi, \omega\pi, \rho\rho, \rho\omega, \omega\omega$ channels are denoted by 0, 3, 4, 4', 5 and 6. Therefore we have the matrix elements M_{i0} with $i = 3, 4, 4', 5$ and 6. For every case we will compute the rate and the one pion energy spectrum. In order to compute the different rates and energy spectra we need to evaluate the quantities: $\sum_{(i)} 1/4 \sum_{\text{spin}} |M_{i0}|^2, \frac{\partial}{\partial k_0} \sum_{(i)} |M_{i0}|^2$ where $\sum_{(i)}$ denotes the i pion phase space integral and $\frac{\partial}{\partial k_0}$ tells us to perform all the integrations except dk_0 . M_{i0} consist of a sum of terms coming from the interchange between pions. If we denote it by $M_{i0} = \sum_j M_{i0}(j)$ then

$$|M_{i0}|^2 = \sum_{jj'} M_{i0}(j)^* M_{i0}(j')$$

Since in $M_{i0}(j)$ we have always a relatively sharp resonance, we will neglect the $j \neq j'$ and then

$$|M_{i0}|^2 = \sum_j |M_{i0}(j)|^2$$

When we perform the phase space integration and carry out the sum over the isotopic spin index, we get the expressions:



$$W^3(\bar{p}p) = W_2^3(\bar{p}p) = 2\pi \times 3 \times 6 \times 12.35 \times 10^{-6} G^2 |A_1 \sqrt{G_2}|^2 \quad (3-1)$$

$$W_1^3(\bar{p}n) = 2\pi \times 4 \times 39.86 \times 10^{-6} G^2 G_2 |A_1 - 0.85 \times 2mB_1|^2 \quad (3.2)$$

$$W_3^3(\bar{p}n) = 2\pi \times 20 \times 39.86 \times 10^{-6} G^2 G_2 |A_1 - 0.85 \times 2mB_1|^2 \quad (3.3)$$

where

$$G_2 = \int_4^{(2m-2)^2} dt_{12} |\exp \Delta(t_{12})|^2 \frac{1}{8\pi} \frac{Q_{12}^3}{t_{12}^{1/2}} \quad (3.4)$$

$$W^3(k; \bar{p}p) = W_2^3(k; \bar{p}p) = 2\pi \times 12.35 \times 10^{-6} G^2 |A_1 \sqrt{G_2}|^2 \times 6 [f_3^{10} + 2f_3^{20}] \begin{pmatrix} 1 \\ 1 \end{pmatrix} \quad (3.5)$$

$$W_1^3(k; \bar{p}n) = 2\pi \times 39.86 \times 10^{-6} G^2 G_2 |A_1 - 0.85 \times 2mB_1|^2 \times 12 [f_3^{11} \begin{pmatrix} 0 \\ 1 \end{pmatrix} + f_3^{21} \begin{pmatrix} 0 \\ 1 \end{pmatrix}] \quad (3.6)$$

$$W_3^3(k; \bar{p}n) = 2\pi \times 39.86 \times 10^{-6} G^2 G_2 |A_1 - 0.85 \times 2mB_1|^2 \times 12 [f_3^{11} \begin{pmatrix} 1 \\ 0 \end{pmatrix} + f_3^{21} \begin{pmatrix} 1 \\ 0 \end{pmatrix}] \quad (3.7)$$

where the vector $\begin{pmatrix} \cdot \\ \cdot \\ 0 \end{pmatrix}$ labels the charge of the pion and means $\begin{pmatrix} + \\ - \\ 0 \end{pmatrix}$.

$$\bar{N} + N \rightarrow \pi + 3\pi$$

$$W^4(\bar{p}p) = W_2^4(\bar{p}p) = 11.57 \times 10^{-6} \times 2\pi \times 24 |\sqrt{G_3} A_2|^2 G^2 \quad (3.8)$$

$$W^4(\bar{p}n) = W_3^4(\bar{p}n) = 2W^4(\bar{p}p) \quad (3.9)$$

where

$$G_3 |A_2|^2 = G_3(t_s) |A_2(t_s)|^2 \quad (3.10)$$

with

$$G_3(t_s) = \frac{1}{12(2\pi)^3} J_0(t_s) \int dt |D(t)|^{-2} \quad (3.11)$$

and

$$I_0(t) = \int_4^{(t^{1/2}-1)^2} dt_{12} \left(\frac{t}{t_{12}}\right)^{1/2} Q_{12}^3 k_3^3 \bar{F}(t_1, t_{12}) \quad (3.12)$$

$$\bar{F}(t_1, t_{12}) = 3/4 \int_{-1}^1 dz (1-z^2) \left| \exp [\Delta(t_{12}) + \Delta(t_{13}) + \Delta(t_{23})] \right|^2 \quad (3.13)$$

$$W_2^4(k; \bar{p}p) = 2\pi \times 11.57 \times 10^{-6} G^2 |A_2 \sqrt{G_3}|^2 \times 24 \left\{ f_4^1(0) + f_4^2(1) \right\} \quad (3.14)$$

$$W_3^4(k; \bar{p}n) = 2\pi \times 11.57 \times 10^{-6} G^2 |A_2 \sqrt{G_3}|^2 \times 48 \left\{ f_4^1(1) + f_4^2(1) \right\} \quad (3.15)$$

$$\bar{N} + N - 2\pi + 2\pi$$

$$W_2^4(\bar{p}p) = 2\pi \times 0.78 \times 10^{-6} \times 4G_2^2 A_1^4 + 2\pi \times 20.64 \times 10^{-6} \times 24G_2^2 f(A_1, B_1) \quad (3.16)$$

$$W_4^4(\bar{p}p) = 2\pi \times 0.78 \times 10^{-6} \times 32G_2^2 A_1^4 \quad (3.17)$$

$$W_3^4(\bar{p}n) = 2\pi \times 20.64 \times 10^{-6} \times 48G_2^2 f(A_1, B_1) \quad (3.18)$$

where

$$f(A_1, B_1) = A_1^4 + 2mB_1 A_1^3 \times 0.934 + (2mB_1)^2 A_1^2 \times 0.227 - \\ - (2mB_1)^3 \times 0.013 - (2mB_1)^4 \times 0.008 \quad (3.19)$$

$$W_2^4(k; \bar{p}p) = 2\pi \times 0.78 \times 10^{-6} G_2^2 A_1^4 \times 12 \times f_4^0(1) + \\ + 2\pi \times 20.64 \times 10^{-6} G_2^2 f(A_1, B_1) \times 24 \times f_4^1(1) \quad (3.20)$$

$$W_4^4(k; \bar{p}p) = 2\pi \cdot 0.78 \times 10^{-6} G_2^2 A_1^2 \times 12 \times f_4^0 \binom{3}{2} \quad (3.21)$$

$$W_3^4(k; \bar{p}n) = 2\pi \times 20.64 \times 10^{-6} G_2^2 f(A_1, B_1) \times 48 \times f_4^1 \binom{1}{1} \quad (3.22)$$

$$\bar{N} + N \rightarrow 2\pi + 3\pi$$

$$W^5(\bar{p}p) = W_4^5(\bar{p}p) = 2\pi \times 0.677 \times 10^{-6} G_2^2 A_1^2 G_3 A_2^2 \times 120 \quad (3.23)$$

$$W^5(\bar{p}n) = W_3^5(\bar{p}n) = 2\pi \times 0.677 \times 10^{-6} G_2^2 A_1^2 G_3 A_2^2 \times 240 \quad (3.24)$$

$$\begin{aligned} W^5(k; \bar{p}p) &= W_4^5(k; \bar{p}p) = \\ &= 2\pi \times 0.677 \times 10^{-6} G_2^2 A_1^2 G_3 A_2^2 \times 120 \left[f_5^1 \binom{1}{0} + f_5^2 \binom{1}{1} \right] \end{aligned} \quad (3.25)$$

$$\begin{aligned} W^5(k; \bar{p}n) &= W_3^5(k; \bar{p}n) = \\ &= 2\pi \times 0.677 \times 10^{-6} G_2^2 A_1^2 G_3 A_2^2 \times 240 \left[f_5^1 \binom{0}{1} + f_5^2 \binom{1}{1} \right] \end{aligned} \quad (3.26)$$

$$\bar{N} + N \rightarrow 3\pi + 3\pi$$

$$W^6(\bar{p}p) = W_4^6(\bar{p}p) = 2\pi \times 0.803 \times 10^{-6} G_3^2 A_2^4 \times 360 \quad (3.27)$$

$$W^6(\bar{p}n) = 0 \quad (3.28)$$

$$W^6(k; \bar{p}p) = W_4^6(k; \bar{p}p) = 2\pi \times 0.803 \times 10^{-6} G_3^2 A_2^4 f_6^1 \binom{1}{1} \times 720 \quad (3.29)$$

IV. COMPARISON WITH THE EXPERIMENTAL CHARGE MULTIPLICITY DISTRIBUTION AND ENERGY SPECTRUM

From the preceding chapter, we see that the computed multiplicities and energy spectra depend on the value of the quantities $G, A_1, \sqrt{G_2}, B_1, \sqrt{G_2}$ and $A_2, \sqrt{G_3}$.

G, A_1, B_1 and A_2 are actually functions of the mass of the particles in the vertex and in particular functions of the mass of the nucleons. Since in our case, one of the nucleons is virtual, the value of these coupling constants may be expected to differ from their value when both nucleons are free.

If we denote by Δ^2 the square of the momentum transfer (minus the square of the mass of the virtual nucleon), then we have:

Table IV-1

Process	$-\Delta^2$	$m^2 + \Delta^2$
1) $\pi + \rho$	$-30.5 \mu^2$	$75.5 \mu^2$
2) $\pi + \omega$	$-28.5 \mu^2$	$73.5 \mu^2$
3) $\rho + \rho$	$-17 \mu^2$	$62 \mu^2$
4) $\rho + \omega$	$-15 \mu^2$	$60 \mu^2$
5) $\omega + \omega$	$-13 \mu^2$	$58 \mu^2$

We see that we are quite far away from the physical nucleon and we should not be surprised if the value of the vertex function is correspondingly different of the value when both nucleons are in the mass shell. We will assume that the value of the coupling constants are the ones for which $m^2 + \Delta^2 = 60$. (This is certainly true for reactions 3), 4) and 5). Although, for the processes 1) and 2), there is perhaps a certain difference, as in these cases the A_3 and B_3 appear multiplied by G , we will absorb this difference in G .

If we define

$$\alpha_1 \equiv A_1 \cdot \sqrt{G_2} \quad \beta_1 \equiv 2mB_1 \sqrt{G_2} \quad \alpha_2 \equiv A_2 \sqrt{G_3} \quad (4.1)$$

we may express the charge multiplicity distribution in terms of G, α_1, β_1 and α_2 .

Before doing it, we would like to know something about the ratio β_1/α_1 . If we assume the ρ particle resonance plays a fundamental role in the nucleon isovector electromagnetic form factor, we find that

$$\frac{\beta_1}{\alpha_1} \simeq \frac{2mG_2^u(0)}{G_1^u(0)} = \frac{2mF_2^u(0)}{F_1^u(0) + 2mF_2^u(0)} = 0.787 \quad (4.2)$$

From 4-1, 2 and the results of the preceding section we may write

$$W_2(\bar{p}p) = 2\pi \times 10^{-4} [2.22 G^2 \alpha_1^2 + 2.777 G^2 \alpha_2^2 + 9.246 \alpha_1^4] \quad (4.3)$$

$$W_4(\bar{p}p) = 2\pi \times 10^{-4} [0.25 \alpha_1^4 + 0.81 \alpha_1^2 \alpha_2^2 + 2.9 \alpha_2^4] \quad (4.4)$$

$$W_1(\bar{p}n) = 2\pi \times 10^{-4} \times 0.173 \alpha_1^2 G^2 \quad (4.5)$$

$$W_3(\bar{p}n) = 2\pi \times 10^{-4} [0.867 G^2 \alpha_1^2 + 5.553 G^2 \alpha_2^2 + 18.49 \alpha_1^4 + 1.624 \alpha_1^2 \alpha_2^2] \quad (4.6)$$

(In $\bar{p}n$ annihilation the model does not allow 5 prongs event, which experimentally constitutes a sizable fraction. See table IV-2)

Table IV-2
Charged Prongs Multiplicity Distribution
(Experimental)

number of prongs	$\bar{p}H$ at rest Horwitz (3a)	$\bar{p}H$ average energy 80 Mev Agnew (3b)	$\bar{p}C$ at rest Agnew (3b)	$\bar{p}D$ at rest Horwitz (3a)	$\bar{n}p$ at 900 Mev Wentzel (3e)
0	2.5%	6%	1.7%	2.9%	

1			14.7%	2.9%	10%
2	40.1%	40%	22.94%	17.6%	
3			30%	29.4%	60%
4	50.6%	49.6%	19.4%	38.2%	
5			10%	9%	30%
6	6.8%	4.4%	1.2%		
number of events	81	135	170	34	

We would like to know what values of G^2 , α_1^2 , α_2^2 are compatible with the observed charge multiplicities. (See table IV-2.)

For both the Horwitz and Agnew experimental data, at rest, one finds $W_2(\bar{p}p)/W_4(\bar{p}p) = 0.805$.

Experimentally we have for the $\bar{p}p$ annihilation cross section $\sigma \sim mb$ at $T = 100$ Mev what yields a value of $0.4 \times 2\pi$ for the transition probability.

If we choose $\alpha_1^2 = 9.3$ $\alpha_2^2 = 26.2$ $G^2 = 10.5$ (this value of G is about a quarter of the one for free nucleons: $G_{free} = 13.4$), then we get

$$W_2(\bar{p}p) = 2\pi \times 0.178$$

$$W_4(\bar{p}p) = 2\pi \times 0.222$$

$$W_2(\bar{p}p) / W_4(\bar{p}p) = 0.8$$

$$W_1(\bar{p}n) = 2\pi \times 0.002$$

$$W_3(\bar{p}n) = 2\pi \times 0.361$$

If we choose different values, namely

$$\alpha_1^2 = 3.2$$

$$\alpha_2^2 = 27.15$$

$$G^2 = 21.13$$

G is about 1/3 of the physical value), then

$$W_2(\bar{p}p) = 2\pi \times 0.178$$

$$W_4(\bar{p}p) = 2\pi \times 0.222$$

$$W_2(\bar{p}n) = 0.8$$

$$W_1(\bar{p}n) = 2\pi \times 0.001$$

$$W_3(\bar{p}n) = 2\pi \times 0.354$$

which is essentially the same result as before. Therefore these results do not depend critically on the value of $G_1 \alpha_1$ and α_2 ; except that if $G/G_{free} > 1/3$ we cannot fit $W_2/W_4 = 0.8$. The preceding values of the parameters lead to the total multiplicities

$$\eta(\bar{p}p) = 4.8 \quad \eta(\bar{p}n) = 4.2$$

Now we will proceed to examine the shape of the energy spectrum. If we substitute the values $\alpha_1^2 = 9.3$ $\alpha_2^2 = 26.2$ $G^2 = 10.5$ in the expressions for the energy spectrum we get

$$W_2(K^\pm; \bar{p}p) = 2\pi \times 10^{-3} \{7.23(f_3^{10} + 2f_3^{20}) + 76.64f_4^2 + 0.807f_4^0 + 79.71f_4^1\} \quad (4.7)$$

$$W_4(K^\pm; \bar{p}p) = 2\pi \times 10^{-3} \{2.42f_4^0 + 19.81(f_5^1 + f_5^2) + 398.66f_6\} \quad (4.8)$$

$$W_1(K^+; \bar{p}n) = 0 \quad (4.9)$$

$$W_1(k^-; \bar{p}n) = 2\pi \times 10^{-3} \times 5.08 f_3^{21} \quad (4.10)$$

$$W_3(k^+; \bar{p}n) = 2\pi \times 10^{-3} \{5.08 f_3^{21} + 143.28 f_4^2 + 159.42 f_4^1 + 39.62 f_5^2\} \quad (4.11)$$

$$W_3(k^-; \bar{p}n) = 2\pi \times 10^{-3} \{5.08 (f_3^{11} + f_3^{21}) + 143.28 (f_4^1 + f_4^2) + 318.84 f_4^1 + 39.62 (f_5^1 + f_5^2)\} \quad (4.12)$$

If however $\alpha_1^2 = 3.2$ $\alpha_2^2 = 27.15$ $G^2 = 21.13$, then the energy spectrum becomes:

$$W_2(k^\pm; \bar{p}p) = 2\pi \times 10^{-3} \{5.01 (f_3^{10} + 2f_3^{20}) + 159.2 f_4^2 + 0.096 f_4^2 + 9.46 f_4^1\} \quad (4.13)$$

$$W_4(k^\pm; \bar{p}p) = 2\pi \times 10^{-3} \{0.29 f_4^0 + 7.56 (f_5^1 + f_5^2) + 426.16 f_6\} \quad (4.14)$$

$$W_1(k^+; \bar{p}n) = 0 \quad (4.15)$$

$$W_1(k^-; \bar{p}n) = 2\pi \times 10^{-3} \times 3.52 f_3^{21} \quad (4.16)$$

$$W_3(k^+; \bar{p}n) = 2\pi \times 10^{-3} \{3.52 f_3^{21} + 318.58 f_4^2 + 18.92 f_4^1 + 15.12 f_5^2\} \quad (4.17)$$

$$W_3(k^-; \bar{p}n) = 2\pi \times 10^{-3} \{3.52 (f_3^{11} + f_3^1) + 318.58 (f_4^1 + f_4^2) + 37.84 f_4^1 + 15.12 (f_5^1 + f_5^2)\} \quad (4.18)$$

In figs. 8 to 15, we plot the preceding energy spectra functions (for both sets of values of the parameters), and compare them with the experimental data. In these curves, the energy spectrum curves corresponding to the first set of parameters are drawn in solid line and the curves corresponding to the second set are drawn

in dashed line.

V. DISCUSSION AND CONCLUSIONS

From the preceding section, we see that both sets of parameters yield a good agreement with the experimental data for the $\bar{p}p$ annihilation energy spectrum, except that the theoretical sharp peak in the two prong events single pion energy spectrum is a little too large. However, better experimental data are needed before reaching a definite conclusion.

In $\bar{p}n$ annihilation, on the other hand, the second set of parameters gives a very huge sharp peak (corresponding to the process $\bar{p} + n \rightarrow \pi^- + \omega$), that is neither reasonable nor observed. If we compare our expression for $W(k; \bar{p}p) + W(k; \bar{p}n)$ with the experimental energy spectrum for the \bar{p} Carbon annihilation (assuming that half of the events are $\bar{p}p$ and the other half $\bar{p}n$), we get a reasonable agreement with the first set of parameters. (We still have a sharp peak which is a little too large). With the second set, the resonance peak is much too large, and therefore, we conclude the first set agrees much better with experiment. However, more experimental data are needed, in order to determine the size of the sharp peaks and to know to what extent the $\bar{N}N$ annihilation process is described by our extreme model.

Since in our model, the charge multiplicity distribution and the energy spectrum are fitted as well in the other extreme model: the statistical model; and since, in the experiments, we observe resonances, we believe that our way of describing the $\bar{N}N$ annihilation process, is perhaps nearer of what actually happens in Nature.

ACKNOWLEDGEMENTS

We would like to express our thanks to Professor R. Blankenbecler for suggesting this problem and for interesting discussions in the different phases of the analysis. We are grateful to Prof. L.R. Cook for several discussions.

REFERENCES

- 1.- O. Chamberlain, E. Segre, C. Wiegand and T. Ypsilantis, *Phys.Rev.* **100**, 947 (1955).
- 2.- B. Cork et al., *Phys.Rev.* **104**, 1193 (1956).
- 3a.- N. Horwitz et al., *Phys.Rev.* **115**, 472 (1959).
- 3b.- L.E. Agnew et al., *Phys.Rev.* **118**, 1371 (1960).
- 3c.- O. Chamberlain et al., *Phys.Rev.* **113**, 1615 (1959).
- 3d.- A.G. Ekspong et al., *Nuclear Physics* **22**, 353 (1961).
- 3e.- W.A. Wenzel in *Proceedings of the 1960 Annual International Conference on High Energy Physics at Rochester*, pp. 155.
- 4.- E. Fermi, *Prog.Theor.Phys.* **5**, 570 (1950).
G. Sudarshan, *Phys.Rev.* **103**, 777 (1956).
- 5.- Z. Koba and G. Takeda, *Prog.of Theor.Phys.* **19**, 269 (1958).
- 6.- J.S. Ball and G.F. Chew, *Phys.Rev.* **109**, 1385 (1958).
- 7.- L.F. Cook and J.V. Lepage, *Phys.Rev.* **120**, 1028 (1960).
- 8.- I. Pomeranchuk, *Doklady Akad. Nauk U.S.S.R.* **78**, 889 (1951).
T. Goto, *Nuovo Cim.* **8**, 625 (1958).
E. Eberle, *Nuovo Cim.* **8**, 610 (1958).
F. Cerulus, *Nuovo Cim.* **14**, 827 (1959).
G. Pinski, preprint.
- 9a.- A.R. Erwin et al., *Phys.Rev. Letters* **6**, 628 (1961), D. Stonehill et al., *Phys. Rev. Letters* **6**, 624 (1961) and E. Pickup et al., *Phys.Rev. Letters* **7**, 192 (1961).
- 9b.- A. Persner et al., *Phys.Rev. Letters* **7**, 421 (1961).
- 10a.- R. Barloutaud et al., *Phys.Rev. Letters* **8**, 32 (1962) and B. Sachi Zarn, *Phys. Rev. Letters* **8**, 282 (1962).
- 10b.- B.C. Maglic et al., *Phys.Rev. Letters* **7**, 178 (1961) and N.H. Xuong et al., *Phys.Rev. Letters* **327** (1961).
- 10c.- B.C. Maglic, preprint.
- 11.- W.R. Frazer and J.R. Fulco *Phys.Rev.* **117**, 1609 (1960).
- 12.- R. Blankenbecler and J. Tarski, *Phys.Rev.* **125**, 782 (1962).

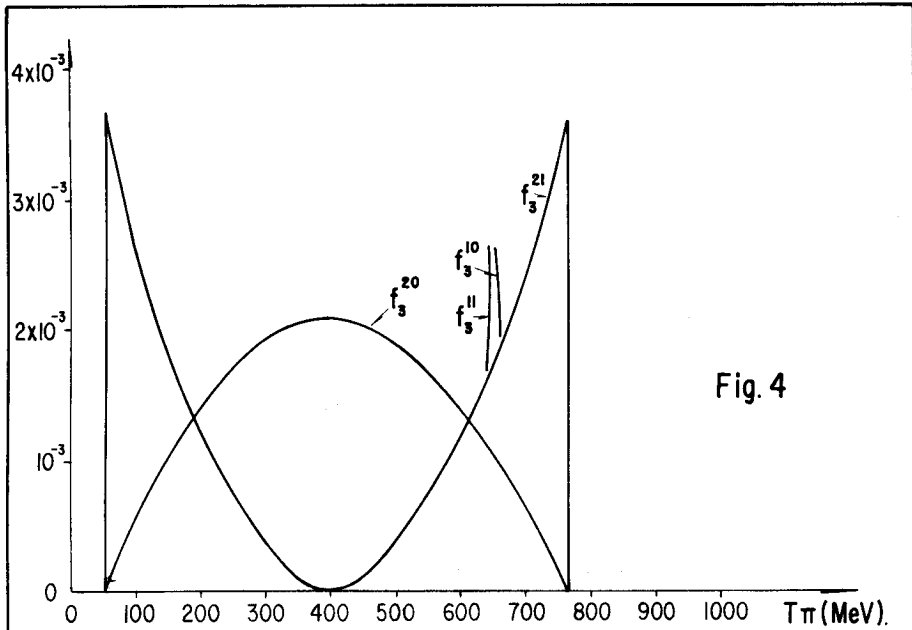


Fig. 4

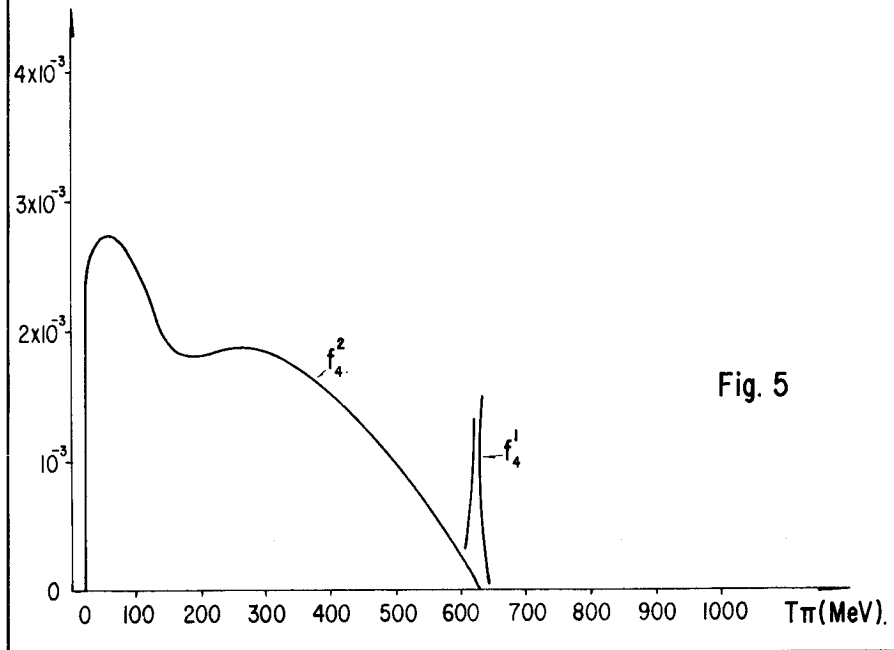


Fig. 5

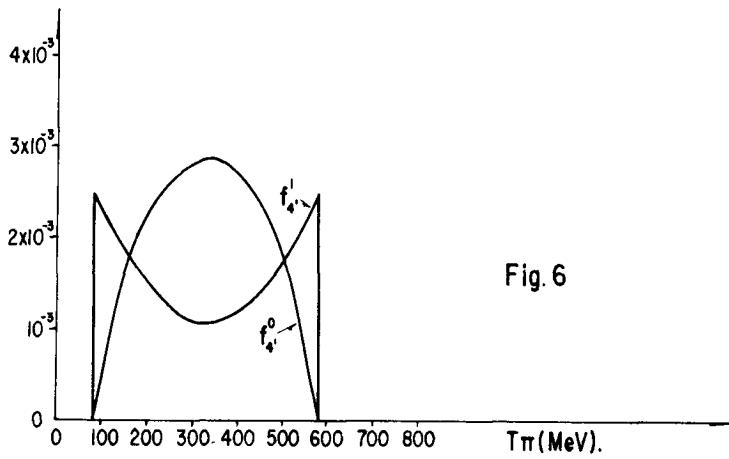


Fig. 6

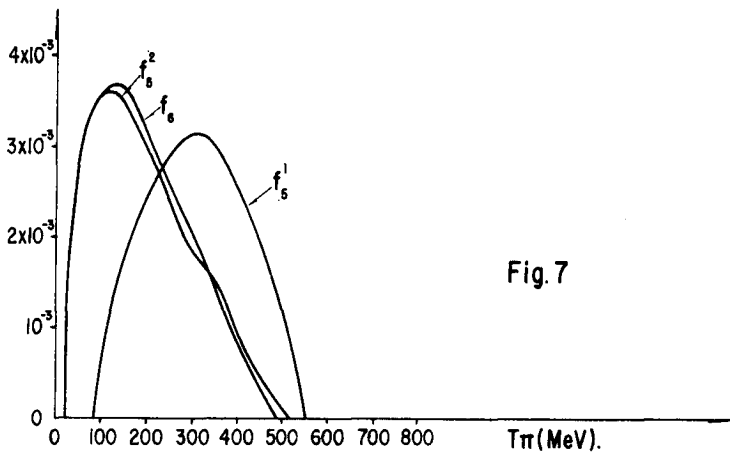


Fig. 7

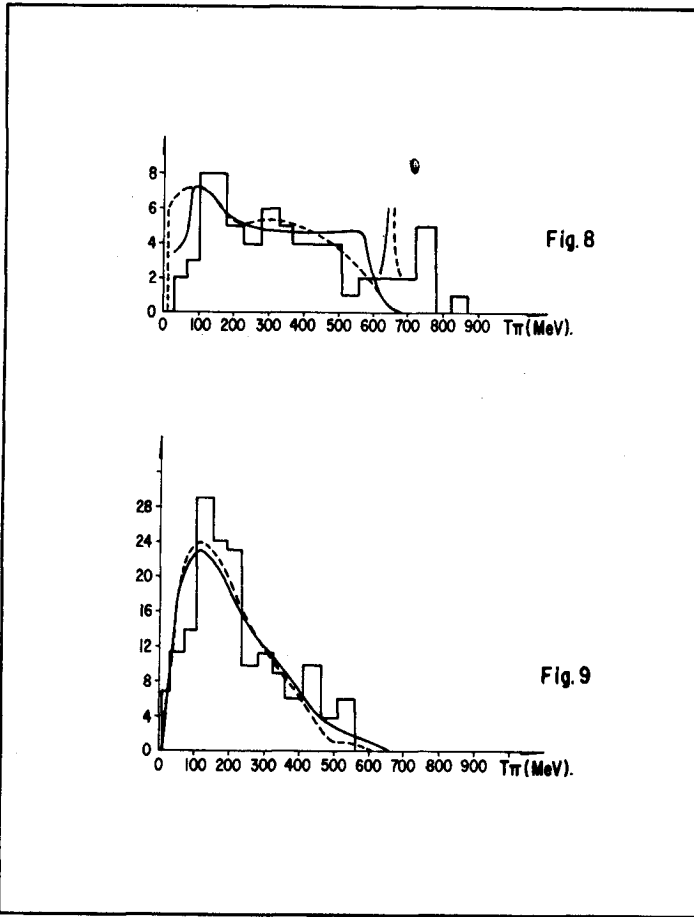


Fig. 8

One pion energy spectrum in 2-prongs $\bar{p}p$ annihilation at rest. The theoretical curve corresponding to the first set of parameters is drawn in solid line and the curve corresponding to the second set is drawn in dashed line. The experimental data are taken from Horwitz et al.^{3a}. The area under the sharp peaks is 42% of the background for the first set of parameters and 2.6% for the second one.

Fig. 9

One pion energy spectrum in 4-prongs $\bar{p}p$ annihilation at rest. (Theoretical curves and Horwitz experimental data).

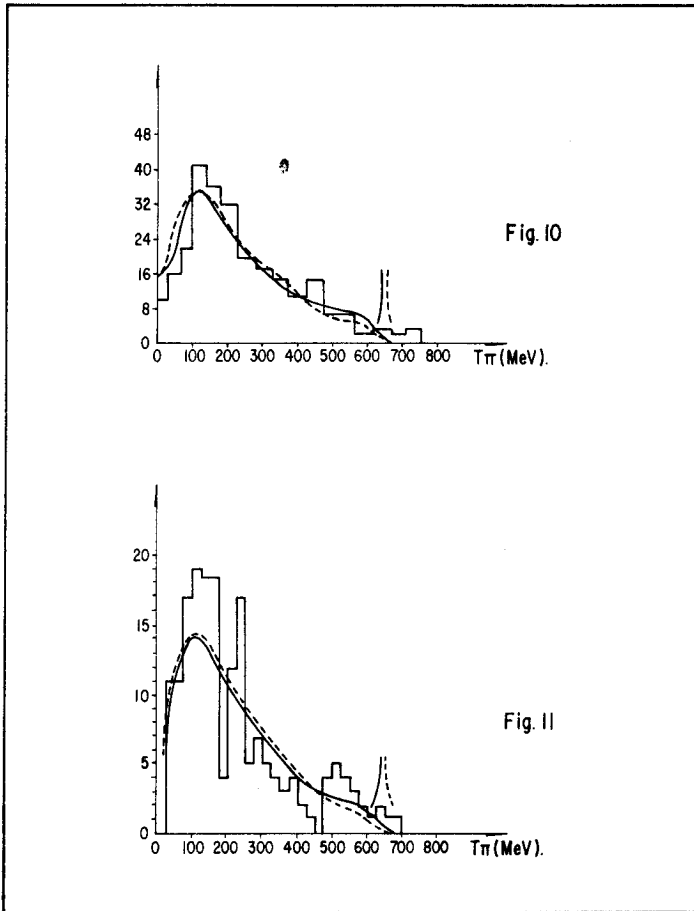


Fig. 10

One pion energy spectrum in $\bar{p}p$ annihilation at rest. (Theoretical curves and Horwitz experimental data).

Fig. 11

One pion energy spectrum in $\bar{p}\bar{p}$ annihilation at rest. (Theoretical curves and Agnew experimental data^{3b}).

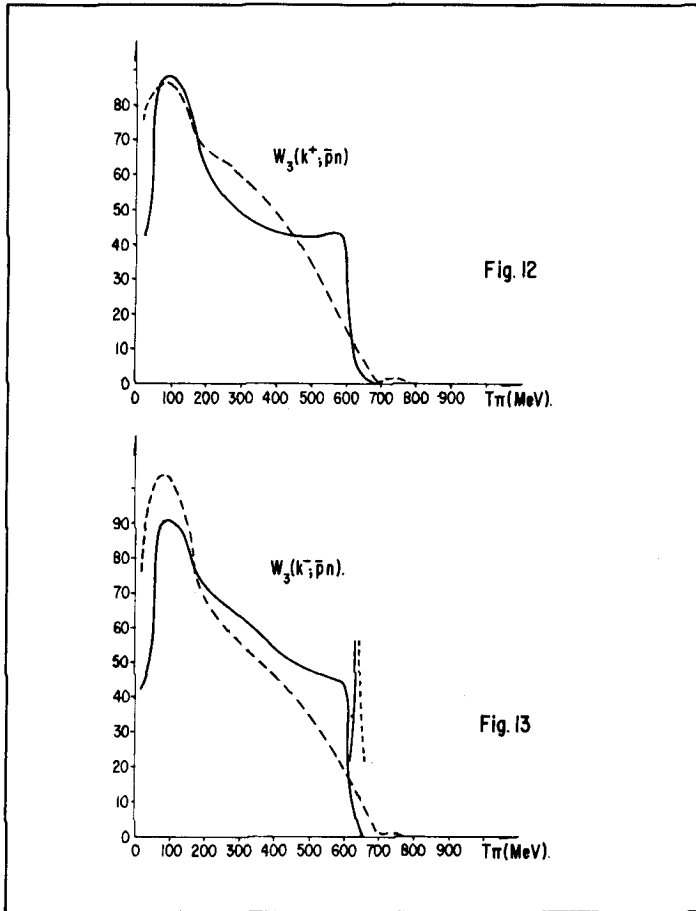


Fig. 12

One positive pion energy spectrum in $\bar{p}n$ annihilation at rest. (Theoretical curves).

Fig. 13

One negative pion energy spectrum in $\bar{p}n$ annihilation at rest. (Theoretical curves). The area under the sharp peak is 25% of the background for the first set and 80% for the second one.

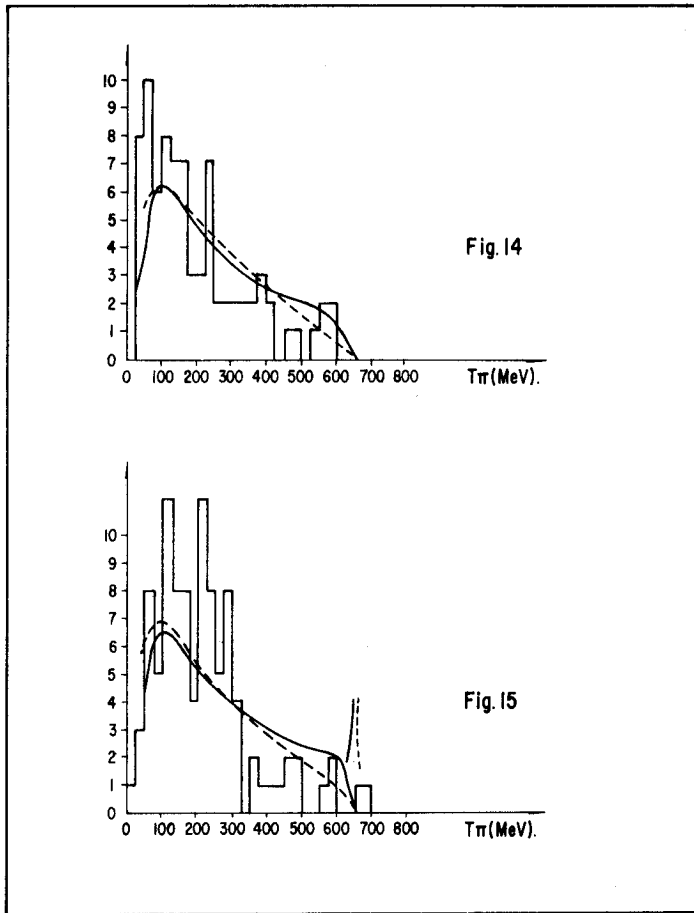


Fig. 14

$W(k^+; \bar{p}p) + W(k^+; \bar{p}n)$ (theoretical) and experimental one positive pion energy spectrum in $\bar{p}C$ annihilation at rest. (Agnew et al^{3b}).

Fig. 15

$W(k^-; \bar{p}p) + W(k^-; \bar{p}n)$ (theoretical) and experimental one negative pion energy spectrum in $\bar{p}C$ annihilation at rest (Agnew et al). The area under the sharp peak is 12% (—) and 35% (----).